REMOTE SENSING OF RAINFALL PARAMETERS BY LASER SCINTILLATION CORRELATION METHOD — NUMERICAL SIMULATION OF THE RETRIEVING

Wu Beiying (吴北婴) and *Lu Daren* (吕达仁)
Institute of Atmospheric Physics, Academia Sinica, Beijing

Received July 18, 1984.

ABSTRACT

This paper is a continuation of an earlier paper[1]. In this paper, we investigate the stability and the representativeness of the rainfall rate h determined by the B_2^*–h relationship in the scintillation method of remote sensing of rain parameters, develop an adequate scheme for retrieving rainfall rate and raindrop size distribution (DSD), and finally characterize the technique by numerical simulations. The results show that the B_2^*–h relationship is quite stable for all the raindrop size distributions used in present simulations; the measured rainfall rate is not severely affected by the distribution of the path-weighting function of B_2^*. The retrieving of DSDs is successful even if the observation errors are assumed in simulations. The rainfall rates derived from the ratrieving of DSD is more accurate than these determined by B_2^*–h relationship. This method is superior in heavier rains.

1. INTRODUCTION

The measurements of rainfall rate and raindrop size distribution (DSD) are of great importance in various fields such as meteorology, hydrology and radio wave propagation etc. Conventional rain-measuring instruments are less representative for mesoscale meteorology because of their very small sampling area and inaccurate sampling time. In 1975, Wang et al.[2] proposed a promising rain-measuring technique making use of the rain-induced scintillations of a laser beam. The instrument they developed gives path-averaged rain parameters with not only much larger sampling area but also better time resolution, nevertheless there are some weaknesses in the derivation and application of their basic equations. In an earlier paper[1], we pointed out the weaknesses and established a set of remote sensing equations in which the measurable quantity, the scintillations of the line-integrated intensity were used. Based on our equations, four ways to obtain rainfall rate have been found and the characteristics of the kernel functions for measuring DSD have been discussed. This paper is a continuation of our earlier work[1]. In this paper, we will deal with some unsolved problems and characterize the technique by various quantitative estimates and numerical simulations. These problems are as follows:

(1) The stability in the measurements of rainfall rate by B_1^*. The change of the shape of DSD will affect the stability of the relationship between the incoherent component of the scintillation and the rainfall rate because rainfall rate is approximately proportional to $a^{3.5}$ whereas the incoherent component B_1^* to a^4, where a is the radius of the raindrop. We will give the range of the B_1^*–h relationship by numerical simulations.

(2) As the incoherent component B_2^* is obtained from an integral over L, the distribution of the path-weighting function will give rise to unequal contributions to B_2^* from drops of the same kind at different distances. Both factors cause errors in retrieving the rainfall rate. These effects will be numerically investigated.

(3) Develop an adequate retrieval scheme and carry out numerical experiments in retrieving the DSD and rainfall rate.

II. BASIC EQUATIONS

The physics of the method will be briefly given here (Reference [1] for details). A raindrop scatters visible light with the phase function concentrating intensively in forward directions. Falling through a horizontal laser beam, the raindrop will induce a transient scattered light pulse (raindrop-induced light scintillation) on the detectors placed in front of the beam (see Fig. 1). Freely falling drops of random distribution within the beam will cause statistical

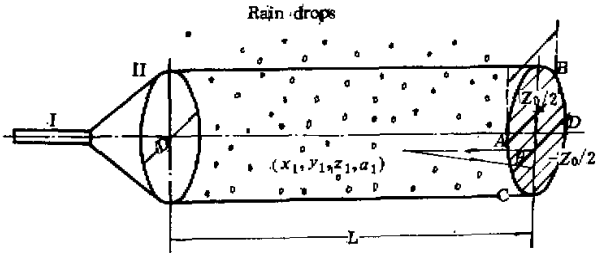

Fig. 1. The geometrical configuration of the experiment in remote sensing of rainfall parameters by laser scintillations. I. a laser; II. the aperture of the transmmitter. AB=CD=l.

scintillations. As the falling velocities of the raindrops of different sizes are different, two detectors seperated vertically at a distance z_0 will receive different scintillation patterns at the same time. These patterns contain the information of the falling raindrops. Therefore it is expected to obtain rain parameters from certain statistical characteristics of the detected light signals. We have deduced in [1] the coherent component B_1^* and the incoherent component B_2^* of the line-integrted intensities received by two detectors, which can be expressed as:

$$B_1^*(z_0,\tau)=\frac{B_1(z_0,\tau)}{I_0^2}=0.2174L\int_0^\infty N_v(a)a^4da\int_0^1 dx^*\int_0^{D/l} dy^*Q$$

$$\times\exp\left\{-0.135Q^2\left(\frac{z_0}{l}-\frac{v\tau}{l}\right)^2\right\}$$

$$\times\{\mathrm{erf}[0.2598Q(1-y^*)]+\mathrm{erf}[0.2598Q(1+y^*)]\}^2$$

$$\times\left\{\mathrm{erf}\left[0.3674Q\left(\sqrt{1+\frac{z_0^2}{l^2}-y^{*2}}-\frac{v\tau}{l}\right)\right]\right.$$

$$\left.+\mathrm{erf}\left[0.3674Q\left(\sqrt{1+\frac{z_0^2}{l^2}-y^{*2}}+\frac{v\tau}{l}\right)\right]\right\}, \qquad (1)$$

$$B_2^*(z_0)=\frac{B_2(z_0)}{I_0^2}=\frac{0.922^2N(N-1)l^2}{2D^4}\left[\int_0^\infty n_v(a)a^2da\int_0^1 dx^*\int_0^{D/l}dy^*I(x^*,y^*,z_0,a)\right]^2$$

$$\simeq\frac{0.922^2\pi^2L^2l^2}{4^2}\left[\int_0^\infty daa^4N_v(a)\int_0^1 dx^*\int_0^{D/l}dy^*I(x^*,y^*,z_0,a)\right]^2,$$

$$I(x^*,y^*,z_0,a)=\left\{\mathrm{erf}\left[0.2598Q\left(\sqrt{1+\frac{z_0^2}{l^2}-y^{*2}}-\frac{z_0}{l}\right)\right]\right.$$

$$\left.+\mathrm{erf}\left[0.2598Q\left(\sqrt{1+\frac{z_0^2}{l^2}-y^{*2}}+\frac{z_0}{l}\right)\right]\right\}$$

$$\times\{\mathrm{erf}[0.2598Q(1-y^*)]+\mathrm{erf}[0.2598Q(1+y^*)]\},\qquad(2)$$

where I_0 is the incident light intensity; z_0 the vertical distance between two detectors; τ the time lag; L the distance between laser and detectors; a the radius of raindrop; $N_v(a)$ is DSD; $n_v(a)=N_v(a)/N_0$, N_0 is the number density of the raindrops; x, y, z are the coordinates defined in Fig.1; v is the terminal velocity of raindrop with radius a; l the length of detectors; D the radius of the cross section of the beam; N the total number of raindrops within the beam at time t. The length is measured in meter and the time in second.

$$x^*=x/L,\ y^*=2y/l,\ z^*=2z/l,\ Q=\frac{ka}{(1-x^*)}\cdot\frac{l}{L}.$$

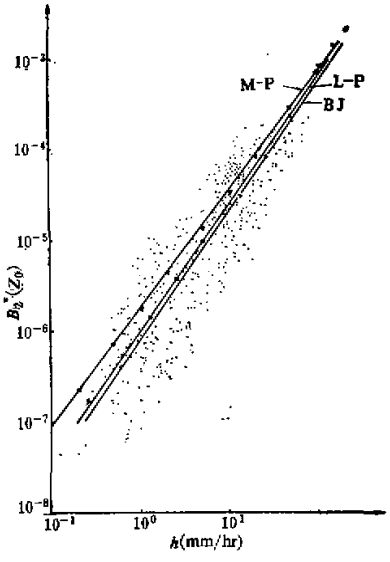

Fig. 2. B_2^*-h relationship for different DSDs. ▲—M-P distribution; ×—L-P distribution; ·—BJ distribution. The solid lines are the regression curves corresponding the distributions as indicated.

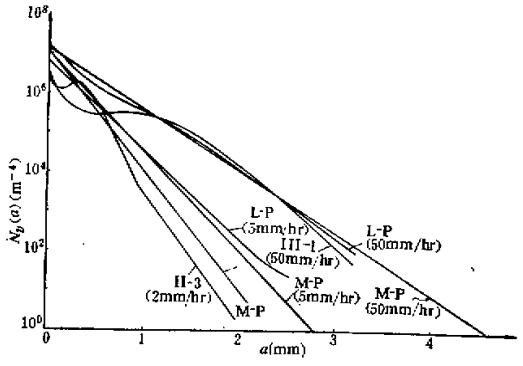

Fig. 3. Some of the DSD used in the numerical simulations.
The rainfall rate for M-P (2nd curve from the left) is 2 mm/hr.

An excellent relationship between B_2^* and rainfall rate h was found through numerical simulation[1]. When DSD is subject to Marshall-Palmer distribution, the relationship is

$$\ln B_2^* = -13.2397 + 1.3158 \ln h. \qquad (3)$$

The correlation coefficient is 0.9998 (the coefficients in (3) are different from those in Fig. 7 of Reference [1], because we adopt here an experimental expression for $v(a)$[3] instead of the approximate one, $v(a) = 200\sqrt{a}$ used in [1]).

B_1^* is related to $N_v(a)$ by

$$B_1^*(z_0, \tau) = \int_0^{a_M} W(z_0, \tau, a) N_v(a) da. \qquad (4)$$

Eq. (4) is a linear integral equation with the kernel function $W(z_0, \tau, a)$. Utilizing the inversion methods in atmospheric remote sensing[4,5], we can obtain the rainfall rate h and DSD from B_1^* and B_2^*.

III. EFFECTS OF THE SHAPE VARIATION OF DSD ON B_2^*

It is clear from Eq. (2) that the incoherent component B_2^* is a functional of DSD, therefore the relationship between B_2^* and h is affected by the shape of DSD. In other words, the relationship (3)deduced from the assumption of M-P distribution may not remain the same accuracy as applied to a rain with DSD of other distributions. In order to investigate the effects,we substituted Marshall-Palmer distribution (M-P distribution) of various rainfall rates, Law-Parsons distribution[6] (L-P distribution) and 289 samples of DSD with the filtering-paper in Beijing (BJ distribution) respectively for $N_v(a)$ to deduce the corresponding B_2^*-h relationships (see Fig. 2). It turns out that the shape of DSD does affect the relationship to some extent. Two conclusions can be drawn from the results shown in Fig. 2:

(1) The B_2^*-h curves derived respectively from L-P and M-P distributions are quite close to each other. Corresponding to the same B_2^*, the relative deviation of the rainfall rates from the two different distributions is about 10% in heavy rains. In light rains the relative deviations are slightly larger but the absolute deviations are not. The relative deviations decrease with increase in rainfall rate. However, the value of B_2^* from L-P distribution is always less than that from M-P distribution. The reason for this can be explained from Fig. 3 as follows. Although the spectral density of L-P distribution is

sometimes slightly larger than that of M–P distribution when the drop radius a is less than a_c, the $N_v(a)$ of L–P distribution vanishes when $a>a_c$ (a_c is the radius of maximum drops in L–P distribution). On the other hand, the $N_v(a)$ of M–P distribution still remains meaningful value when a is larger than a_c. As $B_2^* \propto a^4$ and $h \propto a^{3.5}$, it is expected that B_2^* of L–P distribution will be less than that of M–P distribution at the same rainfall rate.

(2) As for BJ distribution, the relationship between B_2^* and h is rather disperse, which, besides the change of the shape of DSD, is mainly due to the statistical fluctuation caused by the insufficiency in samples. This hardly eliminated by the filtering-paper method with too small sampling areas. The linear regression between ln B_2^* and ln h gives

$$\ln B_2^* = -13.98 + 1.429 \ln h. \tag{5}$$

The correlation coefficient is 0.8725. The parameters in E9.(5) is close to the those for M–P distribution as shown in Fig. 2 (the regression curve from L–P distribution is ln $B_2^* = -13.82 + 1.404 \ln h$).

The above results show that the rainfall rate can be determined from B_2^* with certain accuracy. It is worth pointing out that it is the scintillation method which greatly compresses the dispersion in the results of BJ distribution. The "sampling area" of the scintillation method is 2—3 orders larger than the areas of filter papers, and the sampling time interval is also longer. As a result, the statistical fluctuation in DSD will be deminished, and a more stable B_2^*–h relationship close to our average results can be expected.

IV. PATH REPRESENTATIVENESS OF THE RETRIEVED RAINFALL RATE

B_2^* is derived from the integral with respect to x^*. Therefore the h deduced from B_2^* is path-averaged. We can estimate the contribution of the path-varying rainfall at certain distance from the detectors in the following way. Rewrite Eq. (2) as

$$B_2^*(z_0) = \left\{\int_0^1 dx^* \left[\left(\frac{0.922\pi L l}{4}\right)^2 \int_0^{a_M} da\ a^2\ N_v(a) \int_0^{D/l} dy^* I(x^*, y^*, z_0, a)\right]\right\}^2$$

$$= \left\{\int_0^1 dx^* D(x^*, z_0)\right\}^2, \tag{6}$$

where we assume that $N_v(a, x^*) = N_v(a)$ and $D\ (x^*, z_0)$ represents the contribution of the rainfall rate at x^* to B_2^* (see Fig. 4). It can be seen that $D\ (x^*, z_0)$ is a monotonic function of x^*. The largest contribution always comes from the terminal of the path where the detectors are placed and the smallest at the starting point because the scattered light by a raindrop is attenuated as the scattered light travels farther. Fortunately, the difference between $D\,(1, z_0)$ and $D\,(0, z_0)$ is not very large as shown in Table 1 with the nonuniformity of $D(x^*, z_0)$ described by $\delta D/D$. Thus the rainfall rate can be considered as reasonable average over the whole path. Especially at rainfall rates larger than 10 mm/hr, $D\ (x^*, z_0)$ changes slightly. On the other hand, the rainfall rates below 0.1 mm/hr come mainly from stratiform clouds which distribute very homogeneously over a large area. Therefore the change of the path-weighting function may not severely influence the rainfall rate measured.

Table 1 Nonuniformity of $D\ (x^*, z_0)$

h (mm/hr)	0.1	1	10	100
$\delta D/D$(%)	25.1	15.7	7.86	4.60

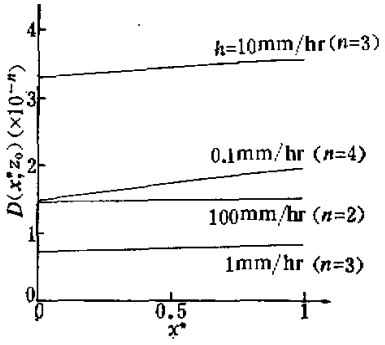

Fig. 4. The path-weighting functions of $B_2^*(z_0)$.

V. NUMERICAL SIMULATIONS

1. *Retrieving Rainfall Rate and DSD by B_1^* and B_2^**

(1) Differentiate the coherent component B_1^* and incoherent component B_2^* from the correlation function $B_f(z_0, \tau)$ of the line-integrated intensities received by the upper and the lower detectors as mentioned in Reference[1].

(2) Make first guess h_0. We have obtained three relationships between B_2^* and h. But as discussed in III, there maybe exist considerable errors in the rainfall rates determined directly from the relationships, no matter which relationship is utilized. However, these relationships are accurate enough to estimate the magnitude of rainfall so that we can select the suitable channels for retrieving. M-P distribution is adopted for this purpose because it is more commonly used than BJ distribution and its analytical form is more convenient to calculate than L-P distribution. Therefore, the first guess h_0 is made from the relationship from M-P distribution.

(3) Divide the first guesses of rainfall rates into four groups: $h<0.5$, $0.5\leqslant h<5$, $5\leqslant h<50$ and $50\leqslant h$, then select the channels $\{B_1^*(z_0,\tau_i)\}$ $i=1, 2, \cdots, M$ and the radial intervel $(0, a_N')$ based on the characteristics of the weighting function $W(z_0, \tau, a)$ in Eq. (4) corresponding to each group.

(4) Calculate the following DSD at rainfall rate h_0:

$$N_v^{(0)}(a)=1.6\times10^7\exp(-8200h_0^{-0.21}a). \tag{7}$$

(5) Form a new weighting function

$$W_N(z_0,\tau,a)=W(z_0,\tau,a)N_v^{(0)}(a) \tag{8}$$

(6) By Phillips-Twomey (P-T) method[4], retrieve the following equation

$$B_1^*(z_0,\tau_i)=\int_{a_0}^{a_M} S(a)W_N(z_0,\tau_i,a)da, \tag{9}$$

and obtain the slowly-varying function $S(a)$.

(7) Finally get the desired quantities

$$\bar{N}_v(a)=S(a)N_v^{(0)}(a), \tag{10}$$

$$h=\frac{4\pi}{3}\int_{a_0}^{a_M} a^3\bar{N}_v(a)v(a)da. \tag{11}$$

The Lagrange multiplier γ in the retrieving is selected as

$$\gamma=\frac{10^{-3}}{\bar{N}}\sum_{j=1}^{N}\|\boldsymbol{a}_j\|^2 \tag{12}$$

with a slightly modification to minimize $(\bar{B}_2^*-B_2^*)/B_2^*$, where N is the numer of the nodes in radius, $a_M=3.5\times10^{-3}$, B_2^* is calculated by substituting the retrieved $\bar{N}_v(a)$ for the $N_v(a)$ in Eq. (2) whereas B_2^* is calculated from the actual $N_v(a)$ assumed. a_j is the column vector of the matrix obtained from discretizing Eq. (9) and $\|\ \|$ symblizes the norm of a vector, defined as $|\mathbf{a}|=\left(\sum_{i=1}^{M}a_i^2\right)^{1/2}$.

2. *Selecting DSD to be Retrieved*

In order to represent the actual DSD we refer to three types of DSD summarized by Gu[17]. They are: Type I, the number density of drop decreases exponentially as radius increases; Type II, a peak of number density locates at the radius varying from 0.15 to 0.25 mm; Type III, occurring in rains heavier than 1 mm/hr, and having two or more peaks in this distribution (the secondary peak is usually at 1 mm or so).

Several functions are applied to imitate the three types. For Type I, M-P distributions at rates h=0.5, 1, 2, 5, 10, 20, 50 100 mm/hr are used. For Type II and III, the following formula is used with different parameters

$$N_v(a)=\begin{cases} a_1(1000a)^a\exp(-1000ba)+a_2\exp(-8200h^{-0.21}a), & (a\neq0)\\ a_1+a_2. & (a=0)\end{cases} \tag{13}$$

The symbols used here are the same as above. The parameters are as follows:

$$\text{I}\text{-}1;\ a=7,\ b=23.2,h=2,a_1=0.9145\times10^{13},\qquad a_2=1.463\times10^6;$$

$$\text{I}\text{-}2;\ a=7,\ b=23.2,h=2,a_1=\begin{cases}0.8249\times10^{13}, & a\neq0\\ 0.8249, & a=0\end{cases}\qquad a_2=2.639\times10^6;$$

$$\text{II}\text{-}3;\ a=7,\ b=23.2,h=2,a_1=\begin{cases}0.9145\times10^{13}, & a\neq0\\ 0.4573, & a=0\end{cases}\qquad a_2=1.463\times10^6,$$

$$\text{III}\text{-}1;\ a=7,\ b=7.8,h=50,a_1=0.7224\times10^9,\qquad a_2=1.155\times10^6,$$

$$\text{III}\text{-}2;\ a=7,\ b=7.8,h=100,a_1=0.1347\times10^{10},\qquad a_2=2.1552\times10^6.$$

3. *Results*

Random errors of normal distribution with a standard deviation of 5% measured values have been added to B_1^* and B_2^* calculated from Eqs. (1) and (2) as the errors in measurements taking into account. The values of B_1^* and B_2^* with errors are regarded as measured data to retrieve the rainfall rate and DSD. The results shown in Table 2 and Fig. 5 indicate that the retrieved rainfall rates h_r in most cases are more accurate than h_0, especially under the condition of non-M-P distribution in heavy rains. The relative errors of the retrieved rainfall rates are generally less than 10% except three cases with Type II distribution which changes more rapidly and deviates greatly from M-P distribution. The errors

are up to 12% in Type II cases. But even in these cases the errors are not too serious to meet the present demand of accuracy in the measurement of rainfall rate.

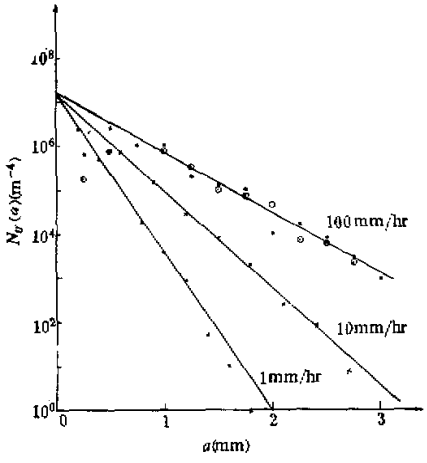

Fig. 5 (a). The retrieved result for M–P distribution.
▲—1 mm/hr; ×—10 mm/hr;
· —100 mm/hr; ◉—100 mm/hr (using another set of channels).

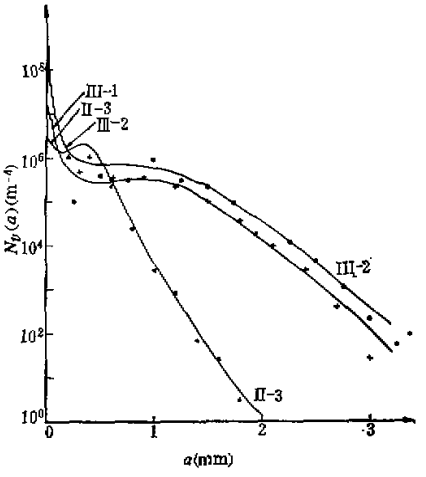

Fig. 5 (b). The retrieved result for non-M–P distributions.
▲—type II-3; ×—type III-1;
· —type III-2.

The average unweighted errors in retrieving DSD are about 40%. Fig. 5 shows that errors are larger at two ends of the radial interval whereas they remain smaller over a wide range between them. As raindrops at the two ends make little contribution to rainfall, the rainfall rate h calculated from the retrieved DSD are not severely affected. Table 2 indicates that the errors weighted by the relative contribution to rainfall have an average value less than 6%. Moreover, it is obvious from Table 2 that in the cases of non-M-P distribution the errors of retrieved distribution are less than that of the initial distribution derived from h_0 according to Eq. (7) and the peak value and its position are re-established quite correctly as seen in Fig. 5 (b). This demonstrates that the retrieved DSD by the present method, to a certain extent, can reflect the deviation of an actual DSD from M–P distribution.

VI. CONCLUSIONS

Based on the numerical simulations of retrieving rainfall rate and DSD and the discussion on some relevant problems described above, the scintillation method can be further characterized as follows:

(1) The relationship B_2^*–h is statistically stable, no matter which distribution in our computation is used. Therefore, rainfall rate h can be roughly determined by B_2^*.

(2) There is a quite uniform path-weighting function in the scintillation method. In heavy rains the path-weighting function changes about 10 % from the initial points of the detecting path to the terminal. Since rainfall can be regarded as uniformly distributed over

Table 2 Results of the Numerical Simulations

Type	h	h_0	h_r	$\Delta h_0/h$	$\Delta h_r/h$	E_0	E_r	E_{0w}	E_{rw}
M-P	0.5	0.4976	0.4996	−0.0048	−0.0008	0.06385	0.5084	0.00092	0.02745
	1.0	0.9714	1.000	−0.0286	0.000	0.05540	0.5291	0.006558	0.01444
	5.0	4.694	4.871	−0.0612	−0.0258	0.07971	0.4341	0.01111	0.02743
	10.0	9.446	9.796	−0.06	−0.0204	0.09941	0.4110	0.01011	0.02037
	20.0	19.09	19.45	−0.0455	−0.0275	0.07029	0.4020	0.04393	0.02150
	30.0	49.15	48.12	−0.017	−0.0376	0.01491	0.4272	0.001726	0.02476
	100.0	103.3	93.99	0.033	−0.0601	0.04752	0.4833	0.005026	0.04825
Ⅱ-1	2.0	2.203	1.756	0.1015	−0.1220	7.413	0.4185	0.1401	0.05874
Ⅱ-2	2.0	2.173	1.779	0.0865	−0.1105	3.822	0.4324	0.005051	0.002180
Ⅱ-3	2.0	2.203	1.756	0.1015	−0.1220	7.522	0.4166	0.005605	0.002349
Ⅲ-1	50.0	22.24	49.07	−0.5552	−0.0186	33.78	0.3563	0.1315	0.02402
Ⅲ-2	100.0	64.05	96.12	−0.3595	−0.0388	1.940	0.4756	0.09433	0.04189

Notes: h is the actual rainfall rate; h_0 is the first guess of rainfall rate; h_r is the retrieved rainfall rate;

$$\Delta h_0/h=(h_0-h)/h,\ \Delta h_r/h=(h_r-h)/h;\quad E_0=\sqrt{\frac{1}{N}\sum_{i=1}^{N}[N_V^{(0)}(a_i)-N_v(a_i)]^2}\ ;$$

E_r is the same as E_0 except that N_{vr} is substituted for $N_V^{(0)}$ (N_{vr} is the DSD which is deduced when h_r is used instead of h_0 in Eq. (7));

$$E_{0w}=\sqrt{\frac{1}{h}\sum_{i=1}^{N}h(a_i)[N_V^{(0)}(a_i)-N_v(a_i)]^2}\ ;$$

E_{rw} is the same as E_{0w} except that N_{vr} is substituted for $N_V^{(0)}$.

a several-hundred-meter path, the effect of the distribution of the path-weighting function on the measurement of rainfall rate is negligible.

(3) It is demonstrated by numerical simulations that the characteristics of several types of DSD can be retrieved even if the sufficient errors in measurements are assumed. Also, the retrieved rainfall rate is more accurate than that from the B_2^*–h relationship.

It should be pointed out that the retrieval accuracy is expected to be further improved by better selection of the channels and the first guess.

We are grateful to Lin Hai who kindly provided us with all the DSD observations and some DSD information used in this paper.

REFERENCES

[1] Wu Beiying and Lu Daren, *Advances in Atmos. Sci.*, 1(1984), 19—29.
[2] Wang T. I. and Clifford S. F., *J. O. S. A*, 65(1975), 927—937.
[3] Gunn R. and Kinzer G. D., *J. Meteo.*, 6(1949), 243—248.
[4] Twomey S., *Introduction to the Methematics of Inversion in Remote Sensing and Indirect Measurements*, Elsevier Scientific Publishing Company, 1977.
[5] 吕达仁，周秀骥，邱金桓， *Scientia Sinca* (*Series B*), XXV(1982), 745—755.
[6] Medhurst R. G., *IEEE. Trans. on Antenna & Propagation*, Ap-13(1965), 550—563.
[7] 顾震潮，云雾降水物理基础，科学出版社，1980，85—86.